

submitted to *Astron. & Asprop.*

# Phase-space Distribution of Volatile Dark Matter.

S. Ghizzardi, S.A. Bonometto\*

Dipartimento di Fisica dell'Università di Milano,  
Via Celoria 16, I-20133 Milano, Italy

I.N.F.N. – Sezione di Milano

## Abstract

We discuss the phase-space distribution of  $\mu$  neutrinos if  $\tau$  neutrinos are unstable and decay into  $\nu_\mu + \text{scalar}$ . If this scalar is a familon or a Majoron, in the generic case the  $\nu_\mu$  background is NOT the straightforward overlap of neutrinos of thermal and decay origins. A delay in  $\nu_\tau$  decay, due to the Pauli exclusion principle, can modify it in a significant way. We provide the equations to calculate the  $\nu_\mu$  distribution and show that, in some cases, there exists a good approximate solution to them. However, even when such solution is not admitted, the equations can be numerically solved following a precise pattern. We give such a solution for a number of typical cases. If  $\nu_\mu$  has a mass  $\sim 2$  eV and the see-saw argument holds,  $\nu_\tau$  must be unstable and the decay into  $\nu_\mu + \text{scalar}$  is a reasonable possibility. The picture leads to a delayed equivalence redshift, which could allow to reconcile COBE data with a bias parameter  $b \geq 1$ .

## 1 Introduction

Cosmological models based on cold dark matter (CDM) allow to approach observational data on large scale structure (LSS) over a wide range of scales. The residual discrepancy between CDM predictions and LSS data can be covered by replacing CDM with a mix of various components, among whom CDM is however the most relevant one. This is in line with the ideas which led to mixed dark matter (MDM) models in the middle eighties [2–5], i.e. that the Universe contains a number of particle species in different

---

\* e-mail:bonometto@astmiu.mi.astro.it

proportions. Most of such species decoupled early and most decoupled components were already non-relativistic when the galaxy mass-scale entered the horizon. Some other component(s) became non relativistic only later on. The former components are CDM and no LSS observation discriminates among them. The latter one(s) will be called *volatile*; among them, *hot* components are characterized by a phase space distribution of thermal origin. Quite at variance from CDM, LSS observations can discriminate among different mixtures of volatile components. As an example, CHDM models with  $\Omega_c = 0.6$ ,  $\Omega_h = 0.3$ ,  $\Omega_b = 0.1$ ,  $g_\nu = 2$  ( $\Omega$  are the usual density parameters; the indeces  $c, h, b$  refer to CDM, hot dark matter, and baryons, respectively;  $g_\nu$  is the number of spin states of the hot component) and C2 $\nu$ DM models with  $\Omega_c = 0.75$ ,  $\Omega_h = 0.2$ ,  $\Omega_b = 0.05$ ,  $g_\nu = 4$  lead to substantially different predictions on a number of statistical estimations, as the expected number of damped  $Ly\alpha$  clouds and the void probability function (VPF) [1]. Another example is given by Pierpaoli & Bonometto [6], who considered different MDM models with a volatile component originating from heavier particle decays, whose transfer functions are substancially different both from CHDM and C2 $\nu$ DM, but still agree with observational constraints for suitable parameters choices.

Heavy particle decays can give origin to volatile components, whose distribution was already studied [7]. A peculiar case however arises when some decay products have the same nature of a pre-existing background of thermal origin. The shape of the resulting distributions can be significantly different from an overlap of thermal and decay components and, for a number of cases, will be discussed in this paper.

A physical context in which such problem is relevant arises if  $\mu$  neutrino has a mass  $\sim 2$  eV [8] and 3 lepton families exist with neutrino masses related by see-saw formulae [9–13]. The  $\tau$  neutrino must then be unstable, not to over-close the Universe (the same argument holds for any value  $m_{\nu_\mu} \gtrsim 0.3$  eV). Its decay into 3 lighter  $\nu$ 's is however unlikely, as – even with weak flavor mixing – it is forbidden at tree-level, unless *ad hoc* models are built. The decay modes  $\nu_\tau \rightarrow \nu_{\mu,e} + e^+ + e^-$ , instead, require that  $m_{\nu_\tau} \gtrsim 1$  MeV and would however seriously modify big-bang nucleosynthesis (BBNS). A decay mode

$$\nu_\tau \rightarrow \nu_\mu + \phi \quad (1)$$

is therefore the most reasonable possibility:  $\phi$  is a scalar particle, arising from the spon-

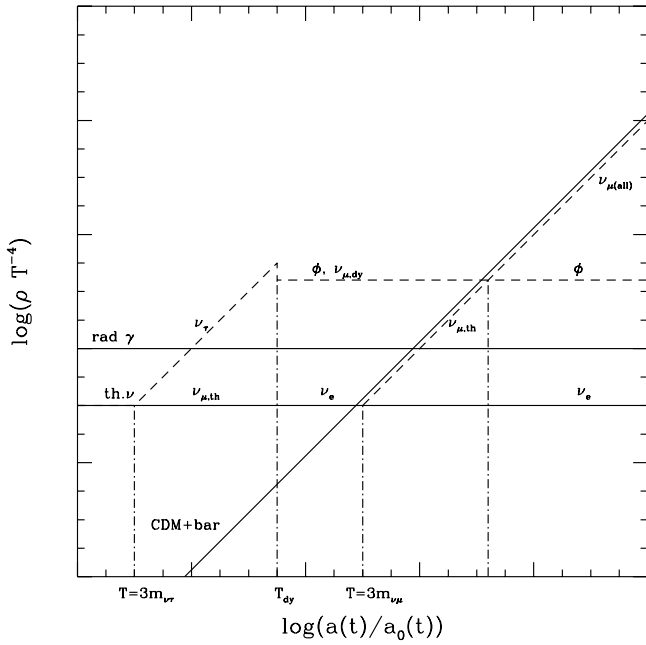


Figure 1: *The energy densities of the different components as functions of the scale factor. In the actual world all “corners” should be smoothed but this qualitative plot outlines: (i) The possible contribution of scalars to the present massless background. (ii) The intermediate behaviour of the two  $\nu_\mu$  backgrounds whose present number density – and, henceforth, energy – is equal. Units on both axes are arbitrary.*

taneous breaking of some global symmetry. Such scalars have been widely considered in the literature. Current examples are Majorons and Familions [13–20].

According to [17], physical parameters are likely to yield a  $\nu_\tau$  life ( $\tau$ ) greater than BBNS age. Accordingly,  $\nu_\tau$  could become non-relativistic only when  $T \lesssim 10$  KeV and decay when the neutrino temperature is  $T_{dy} (\ll m_{\nu_\tau})$ . This does not violate BBNS constraints. Decay yields are  $\nu_\mu$  (possibly, but unlikely, also  $\nu_e$ ) and scalar  $\phi$ 's. When  $\nu_\tau$  decay is essentially over, the Universe contains two “overlapped”  $\nu_\mu$  backgrounds;  $\nu_\mu$  of thermal origin derelativize when  $3T_\nu \simeq m_{\nu_\mu}$ ;  $\nu_\mu$  originated from  $\nu_\tau$  decay derelativize later, when  $T_\nu \simeq m_{\nu_\mu}$  ( $T_{dy}/m_{\nu_\tau}$ ). Furthermore the Universe will contain electron neutrinos, of negligible mass, and massless  $\phi$ 's, which have the same behaviour of massless  $\nu$ 's in the shaping of LSS.

In fig. 1 we plot the typical time dependence of the energy densities of radiation, neutrinos,  $\phi$ 's and non-relativistic components. This figure stresses the fact that

$T_{\nu_\tau,dy}/T_{\nu_\mu,der} \simeq m_{\nu_\tau}/m_{\nu_\mu}$  ( $T_{\nu_\tau,dy}$ : temperature at the time  $\tau$  of  $\nu_\tau$  decay;  $T_{\nu_\mu,der}$ : temperature at  $\nu_\mu$  derelativization).

Such scenario seems the most likely one, if  $m_{\nu_\mu} \sim 2$  eV and masses are related by the see-saw relation. We shall now discuss the shape of the overall  $\nu_\mu$  distribution in this case. This is a typically non-thermal distribution and in the generic cases it is not given by the straightforward overlap of decay and thermal distributions. The final energy of decay  $\nu_\mu$ 's is enhanced by this effect.

## 2 Coupled equations for decaying and daughter particles

The phase space distribution  $f(\mathbf{x}, \mathbf{p}, t)$  of light  $\nu$ 's (both of decay and thermal origin) is obtainable from the Boltzmann equations  $\hat{\mathbf{L}}[f] = \hat{\mathbf{C}}[f]$ , where

$$\hat{\mathbf{L}} = p^\alpha \frac{\partial}{\partial x^\alpha} - \Gamma_{\beta\gamma}^\alpha p^\beta p^\gamma \frac{\partial}{\partial p^\alpha} \quad (2)$$

(greek indeces run from 0 to 3;  $\Gamma$  are Christoffel symbols) and  $\hat{\mathbf{C}}$  is the decay operator. Assuming homogeneity and isotropy, in a Robertson-Walker model with scale factor  $a(t)$ ,  $f$  depends only on  $p^0 = E$  and on the time  $t$ . It is also important to separate the time dependence with occurs because of the decrease of the temperature  $T$  when  $a$  encreases from an actual evolution due to particle events. In general,

$$\hat{\mathbf{L}}[f(E, T)] = E \frac{\partial f}{\partial t} - \frac{\dot{a}}{a} E^2 \frac{\partial f}{\partial E} \quad (3)$$

and, if  $f_{\nu_\tau}$  is the phase-space distribution of the mother particle ( $\nu_\tau$ ), for the decay mode (1),

$$\hat{\mathbf{C}}[f] = 8\pi^4 \int d\Pi_{\nu_\tau} d\Pi_\phi \delta^{(4)}(p_{\nu_\tau} - p_{\nu_\mu} - p_\phi) \left[ |\mathcal{M}_{fi}|_{\nu_\tau \rightarrow \nu_\mu + \phi}^2 f_{\nu_\tau} (1 - f) \right], \quad (4)$$

with  $d\Pi_i = g_i \frac{d\mathbf{p}_i}{(2\pi)^3 2E_i}$  ( $i = \nu_\tau, \phi$ ;  $g_i$  is the number of independent spin-states of the corresponding particle). Assuming  $\tau$  neutrinos at rest, taking  $x = p/T$ , and splitting  $f(x, t)$  into the sum  $f_{dy}(x, t) + fer(x)$  with  $fer(x) = 2/(e^x + 1)$ , eqs. (3) and (4) yield

$$\frac{df_{dy}}{dt}(x, t) = \frac{2\pi^2}{\tau x^2} \frac{n_{\nu_\tau}(t)}{T^3} \delta\left(x - \frac{m_{\nu_\tau}}{2T}\right) (1 - fer(x) - f_{dy}(x, t)) . \quad (5)$$

Here  $n_{\nu_\tau}$  is the number density of  $\nu_\tau$ 's at the time  $t$  and  $\tau = 16\pi m_{\nu_\tau}/|\mathcal{M}_{fi}|^2$  is the  $\nu_\tau$  mean-life, which can be obtained from the decay matrix  $\mathcal{M}_{fi}$  evaluated for  $E_{\nu_\tau} = m_{\nu_\tau}$  and  $p_{\nu_\mu} = p_\phi = m_{\nu_\tau}/2$ . In turn,  $N_{\nu_\tau} = n_{\nu_\tau} a^3$  depends on the decay rate, and is still related to  $f_{dy}$  according to

$$\frac{dN_{\nu_\tau}}{dt} = -\frac{dN_{dy}}{dt} = -\frac{a^3 T^3}{(2\pi)^3} \frac{d}{dt} \int d^3x f_{dy}(x, t) \quad (6)$$

Taking eq. (5) into account, eq. (6) becomes

$$\frac{dN_{\nu_\tau}}{dt} = -\frac{1}{\tau} N_{\nu_\tau}(t) \left[ 1 - fer\left(\frac{m_{\nu_\tau}}{2T}\right) - f_{dy}\left(\frac{m_{\nu_\tau}}{2T}, t\right) \right] \quad (7)$$

If  $fer\left(\frac{m_{\nu_\tau}}{2T}\right)$  and  $f_{dy}\left(\frac{m_{\nu_\tau}}{2T}, t\right)$  are negligible, eq. (7) gives the usual exponential decay and the known  $\nu_\mu$  spectrum. Here we are interested in the opposite case, when such decay-inhibiting terms cannot be disregarded. Neutrinos decoupled at the time  $t_{dg}$  when the temperature was  $T_{dg} \sim 0.9$  MeV. At that time

$$\frac{N_{\nu_\tau}(t_{dg})}{a^3 T^3} = \frac{N_{\nu_\tau}(t_{dg})}{a_{dg}^3 T_{dg}^3} = \frac{n_{\nu_\tau}(t_{dg})}{T_{dg}^3} = \frac{3\zeta(3)}{2\pi^2} \quad (8)$$

and this equation provides us the initial conditions which allow to replace eq. (7) into eq. (5), so obtaining the equation:

$$\begin{aligned} \frac{df_{dy}}{dt}(x, t) &= 6\zeta(3) \frac{\tilde{t}_{dg}}{\tau x} \delta\left(t - \tilde{t}_{dg}x^2\right) (1 - fer(x) - f_{dy}(x, t)) \times \\ &\times \exp\left\{-\frac{1}{\tau} \int_{t_{dg}}^t ds \left[ 1 - fer\left(\sqrt{s/\tilde{t}_{dg}}\right) - f_{dy}\left(x_{dg} (s/t_{dg})^{\frac{1}{2}}, s\right) \right] \right\}. \end{aligned} \quad (9)$$

(here  $x_{dg} = m_{\nu_\tau}/2T_{dg}$  and  $\tilde{t}_{dg} = t_{dg}/x_{dg}^2$ ), whose only unknown is  $f_{dy}$ . Eq. (9) is to be solved for all  $x$ , but is an ordinary differential equation in respect to time. The  $\delta$  function at its r.h.s. allows us to write its formal integral as follows:

$$f_{dy}(x, t) = 6\zeta(3) \frac{\tilde{t}_{dg}}{\tau x} \left\{ 1 - fer(x) - f_{dy}(x, \tilde{t}_{dg}x^2) \right\} \Theta(x - x_{dg}) \Theta(t/\tilde{t}_{dg} - x^2) \times \\ \times \exp \left\{ -\frac{2\tilde{t}_{dg}}{\tau} \int_{x_{dg}}^x du u [1 - fer(u) - f_{dy}(u, \tilde{t}_{dg}u^2)] \right\} \quad (10)$$

(the  $\Theta$ 's are Heaviside step distributions). In general, eq. (7) and (10) can be solved only numerically. However, the non-differential form of (10) allows an easy numerical approach and, in some cases, also an analytical solution can be found. Eq. (10) is one of the results of this work.

### 3 Analytical and numerical solutions

In order to solve eq. (10), let us consider a set of discrete times  $t_n = t_{dg} + n \Delta t$  and the corresponding values  $x_n = x_{dg} \left( \frac{t_n}{t_{dg}} \right)^{\frac{1}{2}}$ . For  $x_n$  in the range set by the Heaviside distributions, eq. (10) yields

$$f(x_n, t_n) = 6\zeta(3) \frac{\tilde{t}_{dg}}{\tau x} (1 - fer(x) - f_{dy}(x_n, t_n)) \times \\ \times \exp \left\{ -\frac{\Delta t}{\tau} \sum_{k=1}^n [1 - fer(x_k) - f_{dy}(x_k, t_k)] \right\} \quad (11)$$

For  $n = 1$ , eq. (11) can be solved by intersecting the curves  $y = f$  and

$$y = 6\zeta(3) \frac{\tilde{t}_{dg}}{\tau x_1} [1 - fer(x_1) - f] \exp \left\{ -\frac{\Delta t}{\tau} [1 - fer(x_1) - f] \right\} \quad (12)$$

(their intersection is unique). Once  $f(x_1, t_1)$  is obtained, we work out  $f(x_2, t_2)$  in a similar fashion, and, eventually, all  $f(x_n, t_n)$ . By reducing the width of  $\Delta t$ , this approach allows any approximation and a straightforward numerical algorithm built on this basis is used to obtain figs. 2. Besides of the solutions obtained for two different parameter choices, these figures also show the distribution obtained from the overlap of a non-inhibited decay component with the thermal one. This shows the significance of the inhibition effects.

Analytical solutions can be found if  $f_{dy}$  can be neglected in respect to  $1 - fer$  and the lifetime  $\tau$  is large enough to yield  $\tau x_{dg}^2/t_{dg} \gg 1$ . In such case eq. (11) is no longer a formal integral, as  $f_{dy}$  appears at the l.h.s. only. Furthermore, taking into account that, for  $y > 0$ ,  $\tanh(y/2) = 1 + 2 \sum_{n=1}^{+\infty} (-1)^n e^{-ny}$  and, henceforth,

$$2 \int_{x_{dg}}^x dy y \frac{e^y - 1}{e^y + 1} = x^2 - x_{dg}^2 - \sum_{n=1}^{+\infty} [Z_n(x) - Z_n(x_{dg})] \quad (13)$$

with  $Z_n(y) = 4(-1)^n \left( \frac{y}{n} + \frac{1}{n^2} \right) e^{-ny}$ , we have that

$$f_{dy}(x, t) = 6\zeta(3) \frac{t_{dg}}{\tau} \frac{1}{x x_{dg}^2} [1 - fer(x)] \exp \left\{ -\frac{t_{dg}}{x_{dg}^2 \tau} \left[ (x^2 - x_{dg}^2) + \sum_{n=1}^{+\infty} [Z_n(x) - Z_n(x_{dg})] \right] \right\} \quad (14)$$

In the exponent the sum can be limited to the first  $N$  terms, provided that  $N x_{dg} \gg 1$ . Such analytical integral is used to obtain fig. 3 in which we report both solutions for two choices of parameters: as it is to be expected, taking greater values of  $\tau$ , the differences become negligible.

## 4 Discussion

The expression (14) yields back the expression obtainable neglecting the preexisting Fermi background, when  $|\sum_{n=1}^{\sim INT(10/x_{dg})} Z_n(x)| \ll x^2$  for any  $x > x_{dg}$  (here  $INT(y)$  indicates the integer nearest to  $y$ ). In fig. 4 we plot the behaviour of  $10 \times |\sum_{n=1}^{3000} Z_n(x)|$  and  $x^2$  (the upper limit is adequate if  $m_{\nu_\tau} \gtrsim 5$  keV and therefore  $x_{dg} \gtrsim 3 \times 10^{-3}$ ). The two curves intersect for  $x \simeq 3$ . At greater  $x$ , the distance between the two curves widens and the inequality holds for any  $x > x_{dg}$  once it is true at  $x_{dg}$ . This implies that the effects of the preexisting background cannot be neglected if the  $m_{\nu_\tau} < 6$  MeV. According to the see-saw relation, if  $m_{\nu_\mu} \sim 2$  eV, the neutrino distribution of thermal origin shall be however taken into account.

In most cases this can be done using eq. (14), which is a fair approximation when  $f_{dy}(x, t) \ll 1 - fer(x)$ , for any  $x \geq x_{dg}$ . The condition is most restrictive at the decoupling itself, where it reads

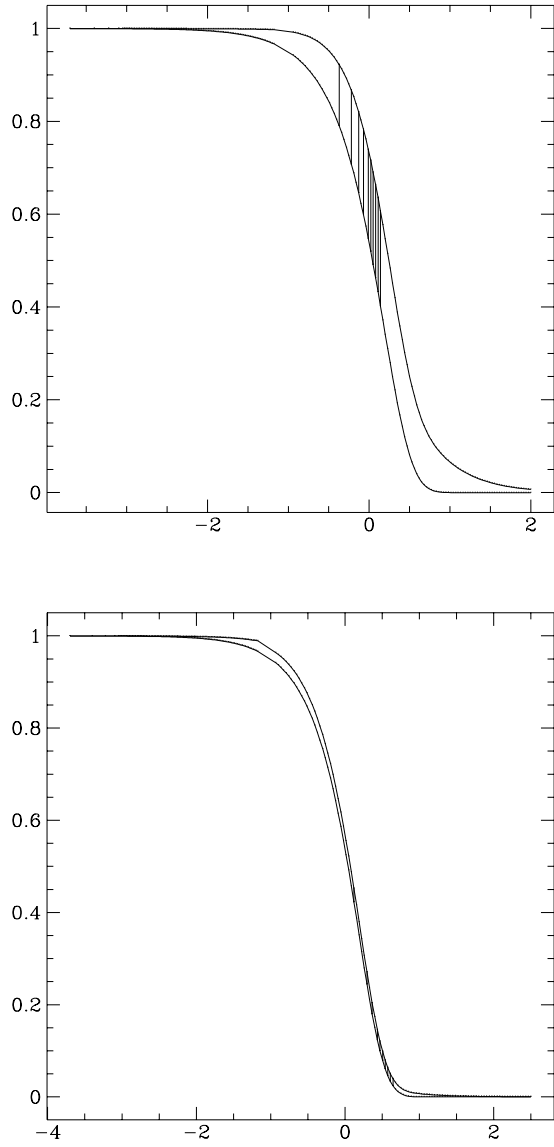


Figure 2: Momentum distribution of  $\nu_\mu$ 's obtained for  $\tau = 10^7$  sec and  $\tau = 10^8$  sec respectively. They are obtained from eq. (10) and through the procedure indicated in eqs. (11) and (12). In practice, no approximation is made here and statistical effects have been considered. In both plots the lower curve represents the preexisting fermi distribution and the upper curve is the total distribution. In the upper plot vertical lines indicate the shape of the spectrum at intermediate times taken at constant time intervals.

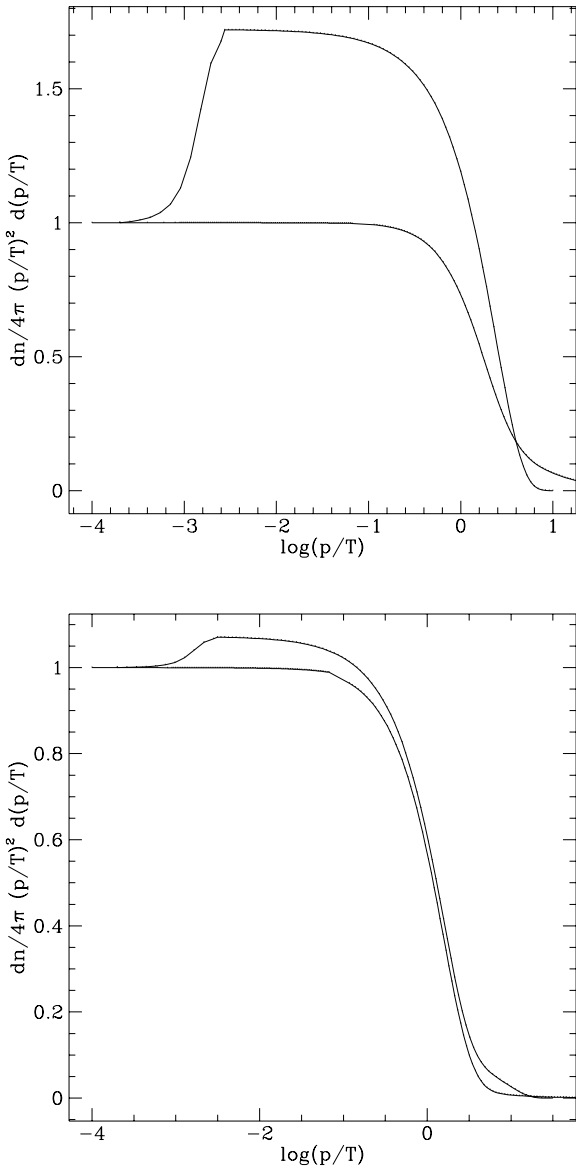


Figure 3: Total momentum distribution of  $\nu_\mu$ 's obtained for  $\tau = 10^7$  sec and  $\tau = 10^8$  sec respectively. They are obtained from eq. (10) (upper plot) and from eq. (14) (lower plot). We compare the real solution with the solution obtained neglecting  $f_{dy}$  in respect with  $1 - fer$ . For high  $\tau$  the differences tend to disappear.

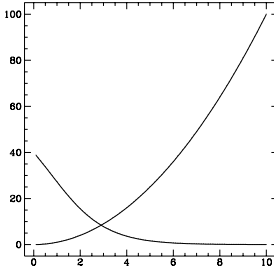


Figure 4: *Intersection between  $10 \times |\sum_{n=1}^{3000} Z_n(x)|$  and  $x^2$ .*

$$\frac{t_{dg}}{\tau} \ll 1.7 \times 10^{-2} \left( \frac{m_{\nu_\tau}}{T_{dg}} \right)^3 \quad (15)$$

or, replacing the values to  $T_{dg}$  and  $t_{dg}$ , known from standard microphysics,

$$\frac{\tau}{\text{sec}} \left( \frac{m_{\nu_\tau}}{4 \times 10^3 \text{ keV}} \right)^3 \gg 1 \quad (16)$$

In the plane  $m_{\nu_\tau} - \tau$  the boundaries of the region where the solution can be approximated by the (14), are represented by the lower dashed line (see fig.5). For parameter choices leading below this curve no approximations can be used. If, for any  $x \geq x_{dg}$ , the inequality  $f_{dy}(x, t) + fer(x) \ll 1$  is satisfied, we can use the exponential solution. In this case, neutrino lifetime is long enough to allow a neglect of the effects of fermi distribution. The inequality, written in terms of  $m_{\nu_\tau}$  and  $\tau$ , becomes:

$$4.8 \times 10^{10} \zeta(3) \left( \frac{\tau}{\text{sec}} \right)^{-1} \left( \frac{m}{\text{keV}} \right)^{-3} + \frac{2}{\exp \left[ 2 \times 10^3 \left( \frac{m}{\text{keV}} \right)^{-1} \right] + 1} \ll 1 \quad (17)$$

This corresponds to the upper dashed-line in fig. 5. Only in the area above this line we can use the exponential solution, neglecting any kind of statistical effect.

In fig. 5 we also show which parameter choices are excluded for various reasons. The area at the right and above the continuous line is excluded in order not to modify the results of the BBNS [21] and in order not to cause drastic changes to the power spectrum of density fluctuations [17]. For permitted values of  $m_{\nu_\tau}$  and  $\tau$  we can make recourse to the approximated solution (eq. (14)) in a few cases, while, in most cases,

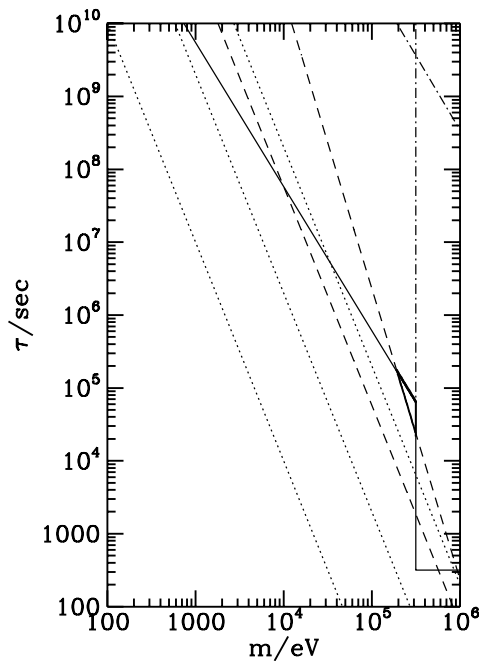


Figure 5: *Excluded region for cosmological reasons is delimited by the continuous line; the dashed line corresponds to the possibility of neglecting some statistical effect. The dotted lines corresponds to eq. (18) for  $V = 10^7, 10^8, 10^9$  GeV.*

the whole solution (eq. (10)) is required. We can also notice that, in the limit of cosmological permitted parameter, the exponential solution can almost never be used. The parameters which permit such a solution are only the ones in the marked triangle in the figure.

According to familon models, once the scale  $V$  of symmetry breaking is known, mass and lifetime of  $\nu_\tau$  decaying into a light neutrino  $\nu_\mu$  and a familon  $\phi$  are related:

$$\tau \simeq 2 \times 10^6 \left( \frac{V}{10^{10} \text{ GeV}} \right)^2 \left( \frac{m_{\nu_\tau}}{\text{keV}} \right)^{-3} \text{ yr} . \quad (18)$$

Eq. (18) yields the curves drawn in fig. 5 (dotted line) for  $V = 10^7, 10^8, 10^9$  GeV. These values of  $V$  are consistent with current theoretical expectations. It is also fair to outline that a self consistent picture arises from their choice. The family symmetry, where spontaneous breaking generates the  $\phi$  scalars, is also consistent with the see-saw argument. Within this scheme, the lifetime of  $\tau$  neutrinos allows them to decay after BBNS and early enough to produce a number of desirable cosmological features. Among them let us outline the increased energy of the low-mass (or massless) backgrounds. This causes a later equivalence redshift (when the energy density of non-relativistic components gets above that of relativistic ones) and therefore rises the expected CMBR fluctuations in respect to fluctuations on the Mpc's scale. In turn, this allows a value of the bias parameter  $b > 1$ . An enhancement of neutrino backgrounds has therefore several appealing features.

In this note we have shown that, if this occurs, the expected neutrino energy distribution can have non trivial features and we have provided the solutions of the equations giving their details. The mechanism acts to delay the decay of heavy neutrinos. Their yields will therefore suffer a smaller redshift and a further enhancement of the decay background shall follow.

## Acknowledgments

We are pleased to thank Antonio Masiero, Marco Roncadelli and Daniela Zanon for helpful discussions.

## References

- [1] S. Ghigna, S. Borgani, S.A. Bonometto, L. Guzzo, A. Klypin, J. Primack, R. Giovanelli, M.P. Haynes, *Astrophys. J.* **437** (1994), L71
- [2] S.A. Bonometto, R. Valdarnini, *Astrophys. J.* **299** (1985), L71
- [3] R. Valdarnini, S.A. Bonometto, *Astron. & Astroph.* **146** (1985), 235
- [4] S. Achilli, F. Occhionero, R. Scaramella *Astrophys. J.* **299** (1985), 577
- [5] J. Holtzmann *Astrophys. J. Suppl.* **71** (1989), 1
- [6] E. Pierpaoli, S.A. Bonometto *Astron. & Astroph.*, (1994) in press
- [7] S.A. Bonometto, F. Gabbiani, A. Masiero *Phys. Rev.* **D49** (1994), 3918
- [8] J.R. Primack, J. Holtzman, A. Klypin, D.O. Caldwell *Nature* (1994),
- [9] G. Gelmini, E. Roulet, preprint UCLA/94/TEP/36– hep-ph/9412278
- [10] T. Yanagida *proc. of the Workshop on Unified Theories and Baryon Number in the Universe. KEK. Japan* (1979)
- [11] M. Gell–Mann, Ramond, R. Slansky *Supergravity* (North Holland 1979)
- [12] R. Johnson, S. Ranfone, J. Schechter, *Phys. Lett.* **B179** (1986), 355;  
R. Johnson, S. Ranfone, J. Schechter, *Phys. Rev.* **B35** (1987), 282
- [13] S.L. Glashow, *Phys. Lett.* **B256** (1991), 218
- [14] G.B. Gelmini, S. Nussinov, T. Yanagida *Nucl. Phys.* **B219** (1983), 31
- [15] F. Wilczek, *Phys. Rev. Lett.* **49** (1982), 1549
- [16] Z. Tao preprint hep-ph 9412223
- [17] M. White, G. Gelmini, J. Silk preprint astro-ph 9411098 CfPA-94-TH-48,  
UCLA/94/TEP/37
- [18] Y. Chikashige, R.N. Mohapatra, R.D. Peccei *Phys. Lett.* **B98** (1981), 265;  
Y. Chikashige, R.N. Mohapatra, R.D. Peccei *Phys. Rev. Lett.* **45** (1980), 1926

- [19] J. Schechter, J.W.F. Valle, *Phys. Rev.* **D25** (1982), 283E;  
J. Schechter, J.W.F. Valle, *Phys. Rev.* **D25** (1982), 774
- [20] G. Gelmini, J.W.F. Valle, *Phys. Rev. Lett.* **B142** (1984), 181;  
K.S.Babu, R.N.Mohapatra, *Phys. Rev. Lett.* **66** (1991), 556
- [21] S.Dodelson, G.Gyuk, M.S.Turner *preprint* astro-ph/9312062, (submitted to *Physical Review D*)